Inorganic Chemistry

Article

pubs.acs.org/IC

Mn^{II}- and Co^{II}-Catalyzed Transformation of 2-Cyanopyrimidine to Methylimidate by Sodium Azide: Isolation, Structural Characterization, and Magnetic Studies on 2D Mn^{II}- and Cu^{II}-Complexes

Malay Dolai,[†] Surajit Biswas,[†] Albert Escuer,[‡] and Mahammad Ali*[,†]

[†]Department of Chemistry, Jadavpur University, 188 Raja Subodh Chandra Mallick Road, Kolkata, West Bengal 700032, India

[‡]Departament de Química Inorgànica and Institut de Nanociència i Nanotecnologia (IN2UB), Universitat de Barcelona, Av. Diagonal 645, 08028-Barcelona, Spain

Supporting Information

ABSTRACT: The Mn^{II}-mediated transformation of 2-cyanopyrimidine to methylimidate in the presence of inorganic azide is proven through isolation and structural characterization of a metal complex. Though the reaction conditions are favorable for a "click" reaction leading to the formation of tetrazole, as evidenced from recent studies, we are astonished to see the formation of methylimidate in MeOH instead of tetrazole, which is supposed to form only in the presence of catalytic amount of corresponding alkoxide ion as base. The catalytic nature of this transformation reaction was confirmed by performing these experiments under catalytic conditions and analyzing the products using liquid chromatography−mass spectrometry techniques, which clearly showed ∼96% and ∼60% selectivity of methylimidate along with almost 100% conversion in the presence of Mn^{II} and Co^{II} as catalysts, respectively. In absence or presence of other metal ions like Cu^{II}, Ni^{II}, Fe^{II}, Zn^{II}, etc. only tetrazole formation takes place. So the present findings extended the formation of methylimidate catalyzed by metal ions in the presence of azide ion in alcoholic medium. Importantly, a probable mechanism for this unexpected transformation was framed based on the structural analysis and high-resolution mass spectrometry (electrospray ionization MS^+) studies. The magnetic studies were also performed on complexes $[Mn(L)(N_3)_2]_n$ (**1**) and $[Cu(L^2)_2]_n$ (**2a**), showing anti-ferromagnetic character for compound **1** and negligible coupling for the copper complex **2a**.

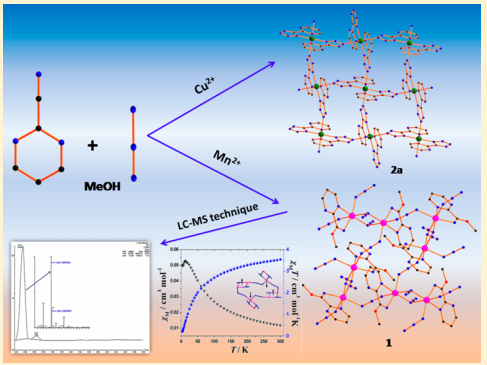

INTRODUCTION

Very recently tetrazole emerges as an important class of compounds[1] with potential applications in (i) medicinal chemistry, material sciences, and pharmaceuticals as lipophilic spacers[2] and carboxylic acid surrogates,[3] (ii) explosives[4] and photography, (iii) information storage technology,[5] and (iv) as precursors for a variety of N-heterocycles[6] and also in coordination chemistry.[7] The usual [2 + 3] cycloadditions of azides and nitriles are found to be the most popular synthetic route to form tetrazoles (Scheme 1). However, evidence in the literature indicates that the mechanism of the reaction is different for different azide species. For example, when an organic azide is used as the dipole, it reacts only with highly activated nitriles as dipolarophiles[8] giving a regioselective 1-alkylated tetrazole,[9] whereas the preparation of 5-substituted 1*H*-tetrazole derivatives involves the addition of inorganic azides to nitriles in a temperature range of typically 100−150 °C. The generation and application of tetrazoles as ligands by one-pot in situ hydrothermal reactions in the presence of transition metal ions have been studied recently.[10] Moreover, Henderson et al. have reported that tetrazoles can be isolated from the reactions of cyanopyridines with sodium azide under ambient conditions within 2−4 h, in the presence of Mn^{II} ion.[11] Interestingly, not many cycloaddition reactions under mild conditions have been reported with first-row transition metal ions.[12]

Scheme 1. Traditional Mechanism of Tetrazole Formation from Nitrile and Azide Ion

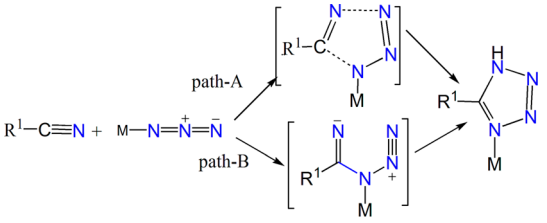

As there are a number of reports on the transformation of nitriles to tetrazoles in the presence of azide ion,[12,13] we intend

Received: May 12, 2015
Published: July 2, 2015

DOI: 10.1021/acs.inorgchem.5b01061
Inorg. Chem. 2015, 54, 7030−7037

Scheme 2. Proposed Synthetic Route for the Formation of Complexes 1 and 2

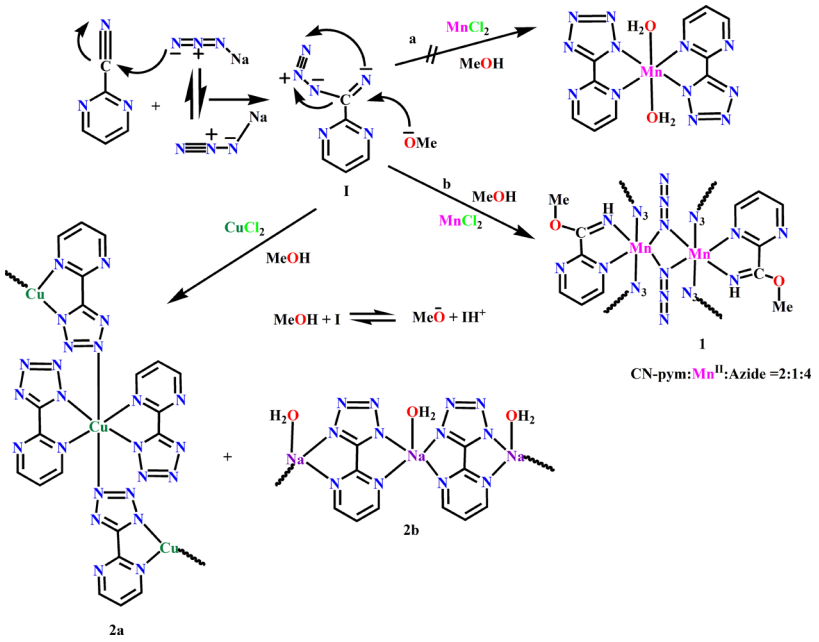

to attempt such a conversion using 2-cyanopyrimidine with Mn^{II} and Co^{II} as well as with other transition metal ions (Cu^{II}, Ni^{II}, Fe^{II}, Zn^{II}, etc.) as catalyst. We are surprised to observe that instead of formation of tetrazole, a rarely investigated methylimidate formation takes place in quantitative yield in methanol as solvent only in the presence of Mn^{II} and Co^{II} ions, while in the presence of other metal ions simple tetrazole formation (Scheme 2) takes place smoothly.

The base-catalyzed formation of alkylimidates through the addition of alcohols to nitriles was discovered by Nef in 1895 (Scheme 3). Shortly thereafter, an easy base-catalyzed

Scheme 3. Alkoxide-Catalyzed Formation of Alkylimidate

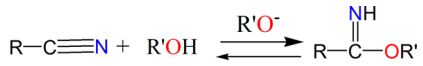

formation of imidates from substituted malononitriles was reported.[14] Later, the reaction of several nitriles with ethanol in the presence of sodium ethoxide were investigated, in considerable extent by Stieglitz,[15] Acree,[16] and others to establish the nature of homogeneous catalysis and to determine the position of equilibrium.[16a] All these studies clearly established that the reactions are alkoxide-catalyzed and that the imidate formation was promoted by the presence of electron-withdrawing groups in the nitriles.[17]

Despite these promising early results,[18−20] virtually no further efforts were paid to elaborate this reaction. So far these reactions go through only in alcoholic medium in the presence of catalytic amount of corresponding alkoxide ion.

In the present article we disclose the formation of a novel methylimidate from 2-cyanopyrimidine, devoid of any electron-withdrawing group, in the presence of azide ion using Mn^{II} and Co^{II} as catalysts, instead of methoxide base. We also explored the effect of different metal ions on this conversion and its catalytic efficacy with the help of electrospray ionization mass spectrometry (ESI-MS^+) spectra and liquid chromatography (LC) MS techniques. It was interesting to note that Mn^{II} and Co^{II} catalyze the formation of methylimidate, while the absence or presence of other metal ions like Fe^{II}, Ni^{II}, Cu^{II}, and Zn^{II} favor the formation of tetrazole (Scheme 4).

Scheme 4. Metal Ion-Catalyzed Formation of Methylimidate and Tetrazole from 2-Cyanopyrimidine

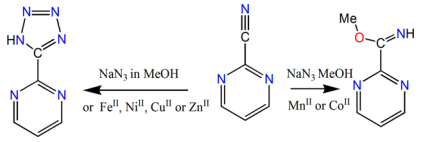

We are fortunate to isolate and structurally characterize a two-dimensional (2D) Mn^{II} coordination polymer formed with methylimidate (Scheme 2) but unfortunate not to be able to get single crystals of corresponding Co^{II} complex. We were also able to isolate and structurally characterize two types of single crystals with tetrazole (vide infra), one with Cu^{II} complex as 2D polymer, while another is one-dimensional (1D) chain of Na^{I} of the same tetrazole ligand when we use Cu^{II} as catalyst.

EXPERIMENTAL SECTION

Materials and Reagents. The starting materials for the synthesis of complexes, $MnCl_2·4H_2O$, $CuCl_2·2H_2O$, sodium azide, and 2-pyrimidine carbonitrile (Aldrich) are of reagent grade and used as received. Solvents like methanol (Merck, India) were of reagent grade and dried before use.

Physical Measurements. Elemental analyses were performed using a Perkin-Elmer 240 elemental analyzer. Infrared spectra (400−4000 cm^{-1}) were recorded from KBr pellets on a Nickolet Magna IR 750 series-II FTIR spectrophotometers. Mass spectra (ESI-MS^+ (m/z)) of the complexes were recorded on Waters high-resolution mass spectrometry (HRMS) spectrometer (model: XEVO-G2QTOF#Y-CA351) interfaced with UPLC facility.

Crystallographic Data Collection and Refinement. The single crystals of compounds **1** and **2** were mounted on the tips of glass fibers with commercially available glue. X-ray data collection of the single crystal was performed at room temperature using Bruker APEX II diffractometer, equipped with a normal focus, sealed tube X-ray source with graphite monochromated Mo Kα radiation (λ = 0.710 73 Å). The data were integrated using SAINT[21] program, and the absorption

DOI: 10.1021/acs.inorgchem.5b01061
Inorg. Chem. 2015, 54, 7030−7037

corrections were made with SADABS.[21] All the structures were solved by SHELXS-97[22] using Patterson method and followed by successive Fourier and difference Fourier map. Full matrix least-squares refinements were performed on F^2 using SHELXL-97[23] with anisotropic displacement parameters for all non-hydrogen atoms. All the hydrogen atoms were fixed geometrically by HFIX command and placed in their ideal positions. Calculations were executed using SHELXS 97,[24] SHELXL 97,[22] PLATON v1.15,[23] TOPOS,[25] and WinGX system Ver-1.80.[26] Data collection and structure refinement parameters along with crystallographic data for complex **1**−**2a** are given in Table 1, and selected bond distances and bond angles of complexes **1** and **2a** are given in Tables 2 and 3, respectively.

Table 1. Data Collection and Structure Refinement Parameters along with Crystallographic Data for Complexes 1 and 2a

parameters	complex **1**	complex **2a**
formula	$C_6H_7MnN_9O$	$C_{10}H_6CuN_{12}$
formula weight	276.15	357.82
crystal system	monoclinic	orthorhombic
space group	$P2_1/c$ (No. 14)	$Pbca$ (No. 61)
a, b, c [Å]	11.0648(4), 9.6507(4),, 10.4244(4)	8.2412(9), 9.5237(11), 17.800(2)
β [deg]	101.145(2)	90
V [Å^3]	1092.16(7)	1397.1(3)
Z	4	16
D(calc) [g/cm^3]	1.679	1.701
μ(Mo Kα) [mm^{-1}]	1.209	6.029
F(000)	556	716
crystal size [mm]	0.18 × 0.25 × 0.35	0.15 × 0.18 × 0.20
temperature (K)	296	296
radiation [λ, Å]	0.710 73	0.710 73
θ min, max [deg]	1.9, 27.2	2.3, 32.1
data set	−14:14 ; −12:12; −13:13	−12:12; −14:14; −26:26
total, unique data, R(int)	9736, 2439, 0.023	19 824, 2365, 0.024
observed data [$I > 2\sigma(I)$]	2185	1658
N_{ref}, N_{par}	2439, 158	2365, 119
R, wR_2, S	0.0237, 0.0729, 1.00	0.0372, 0.1781, 0.70
max and av shift/error	0.00, 0.00	0.00, 0.00
min and max resd dens [e/Å^3]	−0.18, 0.22	−0.47, 0.80

Magnetic Measurements. Magnetic susceptibility measurements were performed on polycrystalline samples using an MPMS-5 Quantum Design SQUID susceptometer working in the range of 30−300 K under an external magnetic field of 0.3 T and under a field of 0.02 T in the 30−2 K range to avoid saturation effects. Magnetization experiments were performed up to 5 T of external field. Diamagnetic corrections were estimated from Pascal's tables.

*Preparation of the Complex $[Mn(L)(N_3)_2]_n$ (**1**).* The one-pot reaction of 2-cyanopyrimidine (2-CN-Pym), $MnCl_2$, and azide ion in 2:1:4 mole ratio in MeOH gives methyl imidate of 2-pyrimidine carbonitrile, which subsequently coordinates to Mn^{2+} to give complex **1**. In a typical procedure 2-CN-Pym (0.104 g, 1.0 mmol) was added to a stirring 20 mL methanolic solution of sodium azide (0.13 g, 2.0 mmol) to give a colorless solution. After a while, $MnCl_2{\cdot}4H_2O$ (0.0985 g, 0.5 mmol) was added to get a brown solution, which was stirred for additional 20 min and then filtered. The resulting brown filtrate with no precipitate was kept aside undisturbed for slow evaporation. After 4 d, the black block-shaped crystals, suitable for X-ray diffraction, were formed. Yield: 0.18 g. (65%). Anal. Calcd. (%) for $C_6H_7MnN_9O$: C 26.09, H 2.55, N 45.65. Found: C 26.12, H 2.49, N 45.68. IR: 2053.3 (s) cm^{-1} for $\nu_{(azido\ bridge)}$, 1641.27 (vs) cm^{-1} for $\nu_{(N=C)}$, 1394(vs) cm^{-1} for $\nu_{(methylimidate)}$.

Table 2. Selected Bond Distances and Bond Angles of Complex 1

bond type	bond length (Å)	bond type	bond angle (deg)
Mn1−N1	2.1925(15)	N3−Mn1−N4	95.70(5)
Mn1−N3	2.2244(15)	N3−Mn1−N7	87.79(5)
Mn1−N4	2.1978(14)	N3−Mn1−N9	159.76(6)
Mn1−N7	2.2985(14)	N3−Mn1−N4^a	91.05(5)
Mn1−N9	2.2282(14)	N4−Mn1−N7	167.99(5)
Mn1−N4^a	2.2838(14)	N4−Mn1−N9	104.24(5)
Mn···Mn separation through the azido (EO) bridge	3.453	N4−Mn1−N4^a	79.22(5)
Mn···Mn separation through the azido (EE) bridge	5.786	N7−Mn1−N9	71.98(5)
bond angles(deg)		N4^b−Mn1−N7	89.25(5)
N1−Mn1−N3	88.93(6)	N4^b−Mn1−N9	89.30(5)
N1−Mn1−N4	93.38(5)	Mn1−N1−N2	136.69(13)
N1−Mn1−N7	98.18(5)	Mn1−N4−Mn1^a	100.78(5)
N1−Mn1−N9	93.29(5)	Mn1b−N4−N5	116.71(11)
N1−Mn−N4^a	172.57(5)	Mn1−N3−N2^c	126.76(12)
Mn1−N4−N5	122.72(12)	Mn1b−N4−N5	116.71(11)

$^a a = 1 - x, -1/2 + y, 5/2 - z$. $^b b = 1 - x, 2 - y, 2 - z$. $^c c = x, 3/2 - y, 1/2 + z$.

Table 3. Selected Bond Distances and Bond Angles of Complex 2a

bond type	bond length (Å)	bond type	bond angle (deg)
Cu1−N1	2.0791(15)	N1^a−Cu1−N3	99.57(6)
Cu1−N3	1.9762(15)	N3−Cu1−N3^a	180.00
Cu1−N5^b	2.3732(17)	N3−Cu1−N5^c	91.98(6)
Cu1−N1^a	2.0791(15)	N1^a−Cu1−N5^b	91.72(6)
Cu1−N3^a	1.9762(15)	N3^a−Cu1−N5^b	91.98(6)
Cu1−N5^c	2.3732(17)	N5^b−Cu1−N5^c	180.00
Cu···Cu separation through μ_3-tetrazolato bridges square grid	6.297	N1^a−Cu1−N3^a	80.44(6)
Cu···Cu separation through the corners of square grid	8.241−9.524	N1^a−Cu1−N5^c	88.28(6)
bond angles (deg)		N3^a−Cu1−N5^c	88.02(6)
N1−Cu1−N3	80.44(6)	Cu1−N3−N4	138.81(14)
N1−Cu1−N5^b	88.28(6)	Cu1^d−N5−N4	119.98(13)
N1−Cu1−N1^a	180.00	Cu1^d−N5−N6	127.11(13)
N1−Cu1−N3^a	99.57(6)	N1−Cu1−N5^c	91.72(6)
N3−Cu1−N5^b	88.02(6)		

$^a c = -x, -y, -z$. $^b b = 1/2 + x, 1/2 - y, -z$. $^c d = -1/2 - x, -1/2 + y, z$. $^d a = -1/2 + x, 1/2 - y, -z$.

*Preparation of the Complex $[Cu(L^2)_2]_n$ (**2a**) and $[Na(L^2)(H_2O)]_n$ (**2b**).* The reaction procedure is same as stated above for the formation of complex **1**, only $CuCl_2{\cdot}2H_2O$ is used instead of $MnCl_2$ $04H_2O$ for the formation of complexes **2a** and **2b**. The color of the crystal of **2a** is blue and greenish-blue for **2b**. Yield: 0.23 g (68%) for **2a**. Anal. Calcd. (%) for $C_{10}H_6CuN_{12}$ (**2a**): C 33.56, H 1.69, N 46.97. Found: C 33.42, H 1.65, N 46.91 for **2a**. IR: 2056.6(s) cm^{-1} for ν(tetrazole), 1622.02(s) cm^{-1} for ν(N═C) for complex **2a**.

Catalytic Studies. We performed the reaction of 2-CN-Pym and sodium azide in 1:2 mole ratio in methanolic medium, in presence of catalytic amount of metal ions (M^{2+} = Mn^{2+} or Co^{2+}). In a typical procedure 2-CN-Pym (0.104 g, 1.0 mmol) was added to a stirring 20 mL methanolic solution of sodium azide (0.13 g, 2.0 mmol) in the round-bottom flask with standard joint to give a colorless solution, and then MCl_2 (0.01 mmol) was added to get light brown solution, which

DOI: 10.1021/acs.inorgchem.5b01061
Inorg. Chem. 2015, 54, 7030−7037

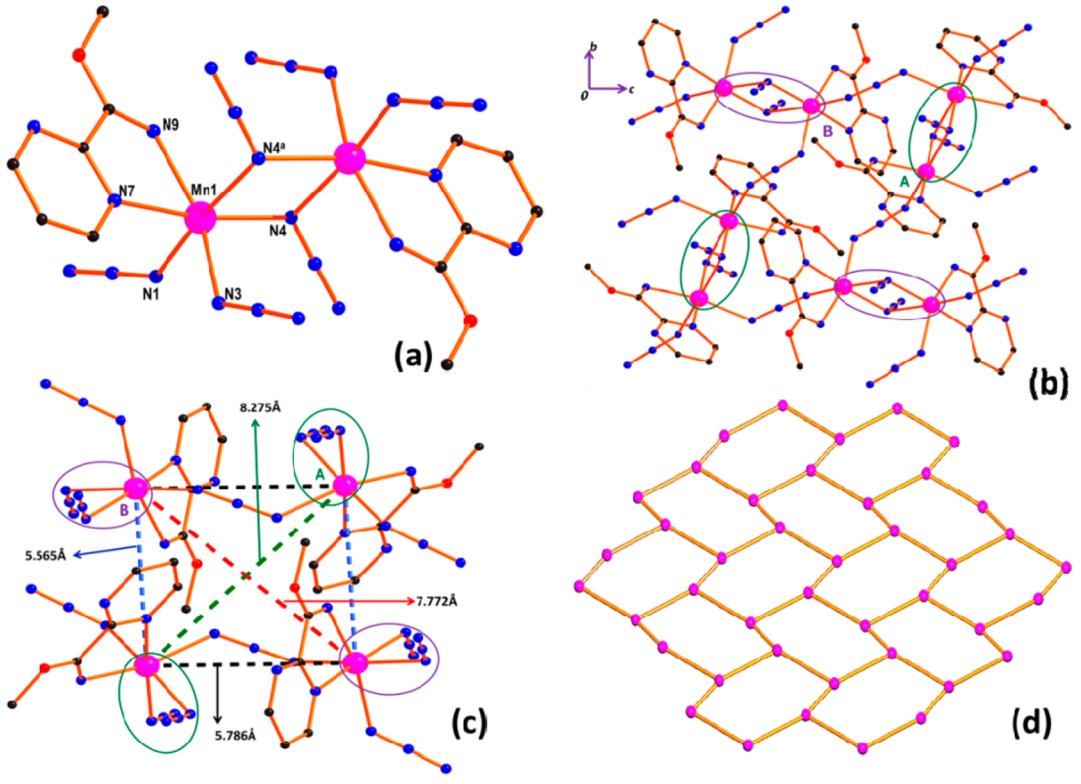

Figure 1. (a) Molecular view along with coordination environment of dimeric unit of **1**. Symmetry code: $a = 1 - x, 2 - y, 2 - z$. (b) 2D framework along the crystallographic *bc* plane and orientations of A and B units in 2D network in **1**. (c) Intermetallic Mn···Mn distances between the dimeric units A and B in 2D network in **1**. All H atoms are omitted for clarity. (d) Topology of uninodal 3-c net with Schläfli symbol $\{6^3\}$ of 2D network of complex **1**.

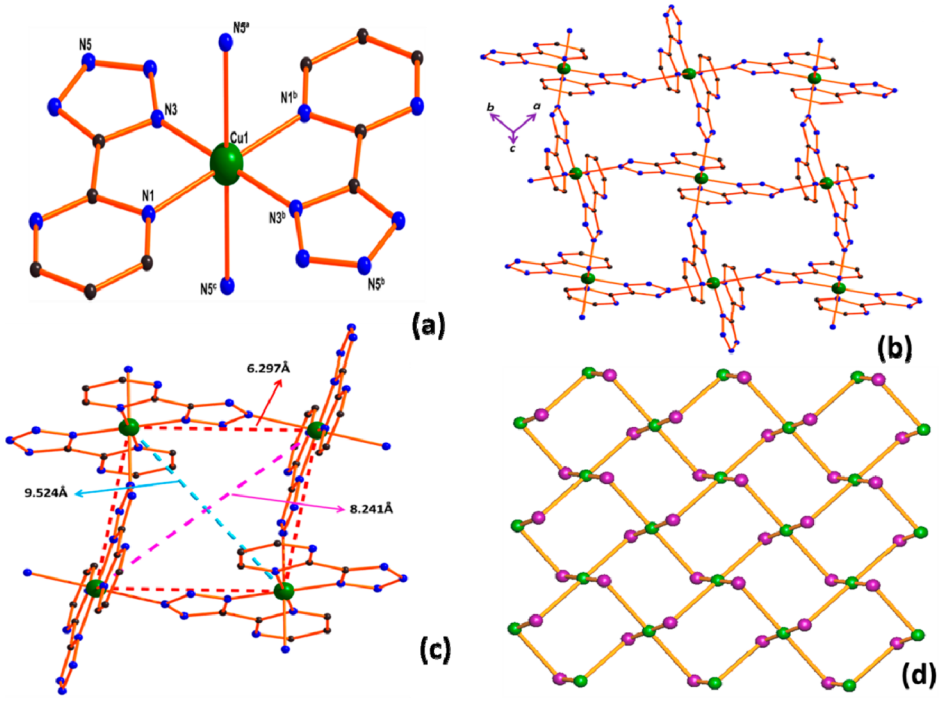

Figure 2. (a) Molecular view along with coordination environment of asymmetric unit of **2a**. Symmetry code: $a = 1/2 + x, 1/2 - y, -z$; $b = -x, -y, -z$; $c = -1/2 - x, -1/2 + y, z$. (b) The 2D framework along the crystallographic *ab* plane in **2a**. (c) Intermetallic Cu···Cu distances shown in the square grid unit in **2a**. All H atoms are omitted for clarity. (d) Topology of binodal 2,4-c net with Schläfli symbol $\{8^4 \cdot 12^2\}\{8\}2$ of 2D network in complex **2a**.

was stirred for further 20 h. Then, the reaction mixture was purified by column chromatography over neutral alumina (mesh 100−150) using an *n*-hexane−ethyl acetate mixture as the eluent to get the desired product layer to separate the metal ions from organic material.

DOI: 10.1021/acs.inorgchem.5b01061
Inorg. Chem. 2015, 54, 7030−7037

Liquid Chromatography–Mass Spectrometry Conditions. The LC conditions adopted are column, acquity UPLC BEH-C18 (2.1 × 50 mm,1.7 μm); solvent A, 0.1% formic acid in water; solvent B, MeCN; flow rate, 0.5 mL/min; injection volume: 5 μL; sample temperature, 10 °C; column temperature: 40 °C; run time, 3 min; seal wash: 5% MeCN in water; purge solvent: 80% MeCN in water with gradient programme (Supporting Information, Table S1).

Mass Spectrometry Conditions. Leucine-enkaphelin (lock spray) in methanol was used as a reference standard, and applied correction is 20 s interval of time.

Other Instrumental Conditions. Mode, ESI-MS$^+$(m/z); analyzer mode, resolution; dynamic range, normal; mass range, 50–1200; scan time, 0.3 s; capillary voltage, 3 kV; sampling cone voltage, 30 V; extraction cone voltage, 3 V; source temperature, 130 °C; desolvation temperatre, 500 °C; cone gas flow rate, 50 L/h; desolvation gas flow rate: 900 L/h.

Results and Discussion. *Crystal Structure Description of [Mn(L)(N$_3$)$_2$]$_n$(**1**).* When 2-pyrimidine carbonitrile and sodium azide in 1:2 mol ratio were reacted in methanol at room temperature in presence of $MnCl_2·4H_2O$ (0.5 equiv), a dark brown solution resulted, which on slow evaporation at ambient temperature yields dark brown single crystals suitable for X-ray diffraction. The X-ray diffraction studies reveal that complex **1** crystallizes in a *monoclinic* system with $P2_1/c$ space group. In the Mn(II) dimers, the two metals are symmetry related over an inversion center and bridged by two $\mu_{1,1}$-azides though N4 and N4^a as shown in Figure 1a. The asymmetric unit consists of one Mn(II) ion, one pyrimidine-2-methylimidate (L), and two azide ions (one $\mu_{1,3}$ and one $\mu_{1,1}$), the latter being involved to expand this asymmetric unit into a 2D layer in which doubly $\mu_{1,1}$ azido-bridged dimanganese(II) units are joined by single $\mu_{1,3}$-azido bridges along the crystallographic *bc* plane (Figure1b). Each Mn center is in octahedral geometry coordinated by N7 and N9 from pyrimidine-2-methylimidate, N1, N3 ($\mu_{1,3}$-N$_3$), and N4 and N4^a ($\mu_{1,1}$-N$_3$) linkers from the four coordinated azide ions (symmetry code: (a) $-x$, 1/2 + y, 1/2 − z). The Mn^{II}–N7/N9 bond lengths fall in range of 2.229(2)–2.300(2) Å along with Mn–N (azido) distances of 2.198 and 2.284 Å. In the Mn_2N_2 planar ring, the Mn–N–Mn bridging angle is 100.78(5)°, and the Mn···Mn separation through $\mu_{1,1}$ and $\mu_{1,3}$-N$_3$ bridges are 3.453 Å and 5.786 Å, respectively. The adjacent {Mn$_2$–N$_{azido}$} planes are nearly parallel to each other with dihedral angle of 10.22° in the 2D framework. The bridging azides are almost linear with the N1–N2–N3 and N4–N5–N6 angles of 177.53° and 178.95(19)°, respectively. In the 2D network, there are two types of dimeric units, which are designated by A and B. Now, two A and two B dimers constitute a rhombus-like framework where each corner of the rhombus is being occupied by A and B alternatively. In this context, there are two different Mn···Mn distances in A to B dimers, namely, 5.565 and 5.786 Å. Again, B to B and A to A Mn···Mn distances along the corners of the rhombus are 7.772 and 8.275 Å, respectively (Figure 1c). The topology of 2D network suggests that **1** is of uninodal 3-c net with Schläfli symbol {6^3} (Figure 1d). The polyhedral representation of **1** as shown in Supporting Information, Figure S1 is a 2D arrangement. There are strong H-bonding and anion-π interactions present in complex **1** (Supporting Information, Figure S2).

*Structural Description of [Cu(L^2)$_2$]$_n$ (**2a**).* The reaction condition is same as that used in the synthesis of the complex **1**, only $CuCl_2·2H_2O$ (0.5 equiv) is used instead of $MnCl_2$. The resulting green solution was filtered, which on slow evaporation at ambient temperature yields blue color single crystal suitable for X-ray diffraction. A single-crystal X-ray diffraction study reveals that complex **2a** is a 2D coordination polymer crystallized in *orthorhombic* system with *Pbca* space group. As shown in Figure 2a, the asymmetric unit of **2a** is composed of one hexacoordinated Cu^{II} center in roughly octahedral geometry. The equatorial plane is being occupied by two pyrimidine 2-tetrazolate ligands (L^2), and two axial positions are occupied by two neighboring tetrazolyl (μ_3) N donor atoms, which expand this asymmetric unit into a 2D architecture (Figure 2b) via $\mu_{1,3}$-tetrazolyl coordination modes; this seems to be quite different from the previously reported results[13] where Cu^{II} center is hexacoordinated with three pyrimidine 2-tetrazolate ligands (L^2) that form an overall 2D (6,3) honeycomb structure. Each Cu^{II} center is in octahedral geometry, coordinated by N1, N1^b, N3, and N3^b (b = $-x$, $-y$, $-z$) from two pyrimidine 2-tetrazolate and two tetrazolyl ($\mu_{1,3}$) nitrogen atoms N5^a, N5^c (a = 1/2 + x, 1/2 − y, $-z$; c = $-1/2$ − x, $-1/2$ + y, z). The Cu^{II}–N1/N3 bond lengths fall in the range of 1.9762(15)–2.0791(15)Å along with Cu–N5 ($\mu_{1,3}$-tetrazolato) distance of 2.3732(17) Å. In the 2D network, there are square grids formed through $\mu_{1,3}$-tetrazolato bridging. In this context, the Cu···Cu separations in the square grid (Figure 2c) are 6.297 Å, and this separation through the corners of the square are 8.241 and 9.524 Å, respectively. The topology of 2D network suggests that **2a** is of binodal 2,4-c net with Schläfli symbol {8^4·12^2}{8}2 (Figure 2d). The polyhedral representation of **2a** as shown in Supporting Information, Figure S3 is a 2D arrangement. The purity of complex **2a** was checked by means of powder X-ray diffraction analysis (Supporting Information, Figure S4). The other 1D chain, [Na(L^2)-(H$_2$O)]$_n$ (**2b**) (Supporting Information, Figure S5), with Na(I) is already reported in the literature,[27] and we are loath to elaborate discussion on it.

Magnetic Studies. Room-temperature $\chi_M T$ value for compound **1** is found to be 3.54 cm^3 mol^{-1} K, and lower than the value for an isolated Mn^{II} cation (4.375 cm^3 mol^{-1} K), and it decreases continuously when the sample is cooled. On further lowering the temperature, χ_{MT} value tends to zero, and χ_M plot exhibits a well-defined maximum at 12 K, evidencing anti-ferromagnetic overall character (Figure 3).

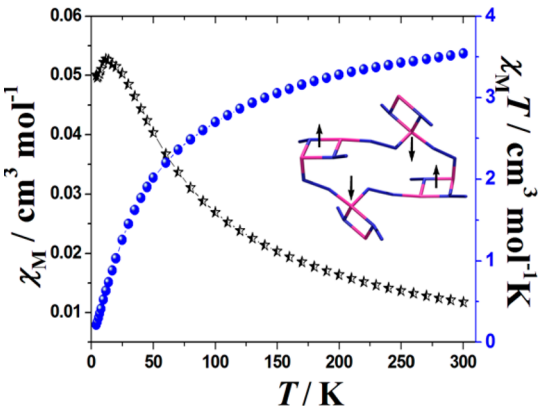

Figure 3. Temperature dependence of χ_M (stars) and $\chi_M T$ (spheres) for **1**. The full lines correspond to the best fit of the data.

According to the structural data (Table 4), the compound should be envisaged as pairs of Mn^{II} cations bridged by $\mu_{1,1}$-N$_3$ ligands and linked between them by means of $\mu_{1,3}$-N$_3$ bridges. Double end-on azido bridges with Mn–N–Mn bond angles around 100° induce ferromagnetic interactions, typically <5 cm^{-1}.[28a] In contrast, end-to-end azido bridges promote anti-ferromagnetic interactions in a wide range of J values as a function of the bond parameters: maximum anti-ferromagnetic interactions should be found for moderate Mn–N–N bond angles (120°–135°) and zero Mn–NNN–Mn torsion angle, whereas weaker interactions are expected for large bond angles and/or 90° torsion.[28b]

In our case, the Mn–N–N bond angles lie in the usual range, but the Mn–NNN–Mn torsion angle is 89.9°; thus, the expected anti-ferromagnetic interaction should be relatively weak. The overall magnetic response is dependent either on the sign of the local interactions or on the topology of the system. In complex **1**, each local S = 5 derived from the ferromagnetic interaction inside the Mn–($\mu_{1,1}$-N$_3$)$_2$–Mn fragments interact anti-ferromagnetically between them through μ-$_{1,3}$ azide bridges in a square arrangement (Figure 3, inset), and then a bulk anti-ferromagnetic response should be expected. Calculation of the Weiss constant from the $1/_{\chi M}$ versus T plot gives a value of −54.7 K confirming the anti-ferromagnetic interaction. Canting phenomenon has been reported in some cases for systems with related topology,[29] but measurements performed below 30 K at low field (0.02 T) do not show spin-canting or other large-order

DOI: 10.1021/acs.inorgchem.5b01061
Inorg. Chem. 2015, 54, 7030–7037

Table 4. Bond Angles (deg) and Lengths (Å) and Magnetic Parameters of All the Mn(II)-Azide Compounds Containing Double $\mu_{1,1}$-N_3 and Single $\mu_{1,3}$-N_3 Bridges[a]

compound	Mn−$N_{1,1}$−Mn	Mn−$N_{1,1}$	Mn−$N_{1,3}$−N	Mn−$N_{1,3}$	$J_{1,1}$ (cm^{-1})	$J_{1,3}$ (cm^{-1})	ref
$[Mn(mptz)(N_3)_2H_2O]$	101.7	2.277	146.4	2.174	0.99	−5.91	30
		2.323	138.2	2.178			
$[Mn_2(3\text{-Et,4-Mepy})_6(N_3)_2(N_3)]_n^{n+}$	101.4	2.207	150.5	2.164	3.3	−5.16	31a
$[\{Mn_2(3ampy)_4(N_3)_4(H_2O)4H_2O\}_n]$	99.6	2.214	133.1	2.188	2.3	−6.01	31a
		2.280					
$[Mn(4\text{-N3py})_2(N_3)_2]_n$	99.7	2.230	125.2	2.205	>0	<0	32
		2.231	137.9	2.180			
		167.5	2.185				
		127.2	2.202				
$[\{Mn(PMK)(N_3)_2\}_n]$ [b]	96.5	2.209	146.5	2.127			31b
$[Mn_3(PMKA)_2(N_3)_6]_n$ [b]		2.289	137.6	2.169			33
$[\{Mn(PMK)(N_3)_2\}_n]\cdot MeOH$ [b]	96.2	2.224	130.4	2.134			31b
$[Mn_2(PMK)_2(N_3)_3]_n(ClO_4)_n\cdot nH_2O$		2.269	140.8	2.180			33
$[\{Mn(dmbpy)(N_3)_2\}_n]$	102.2	2.203	153.9	2.223	1.7	−5.4	31c
		2.337	163.8	2.147			
$[Mn_2(bpym)(N_3)_4]$	104.5	2.215	161.3	2.177	>0	<0	34
		2.230	126.6	2.216			
$[Mn(azpy)(N_3)_2]_n$	103.9	2.188	136.3	2.176	0.1	−4.2	35
		2.189	145.9	2.158			
$[Mn(pymimd)(N_3)_2]_n$(**1**)	100.7	2.198	136.6	2.192	>0	<0	this work
		2.284	126.7	2.224			

[a]Only compounds present the same topology as compound **1**. [b]Besides the double $\mu_{1,1}$-N_3, there is an additional −N−N− bridge in the Mn(II) dimer.

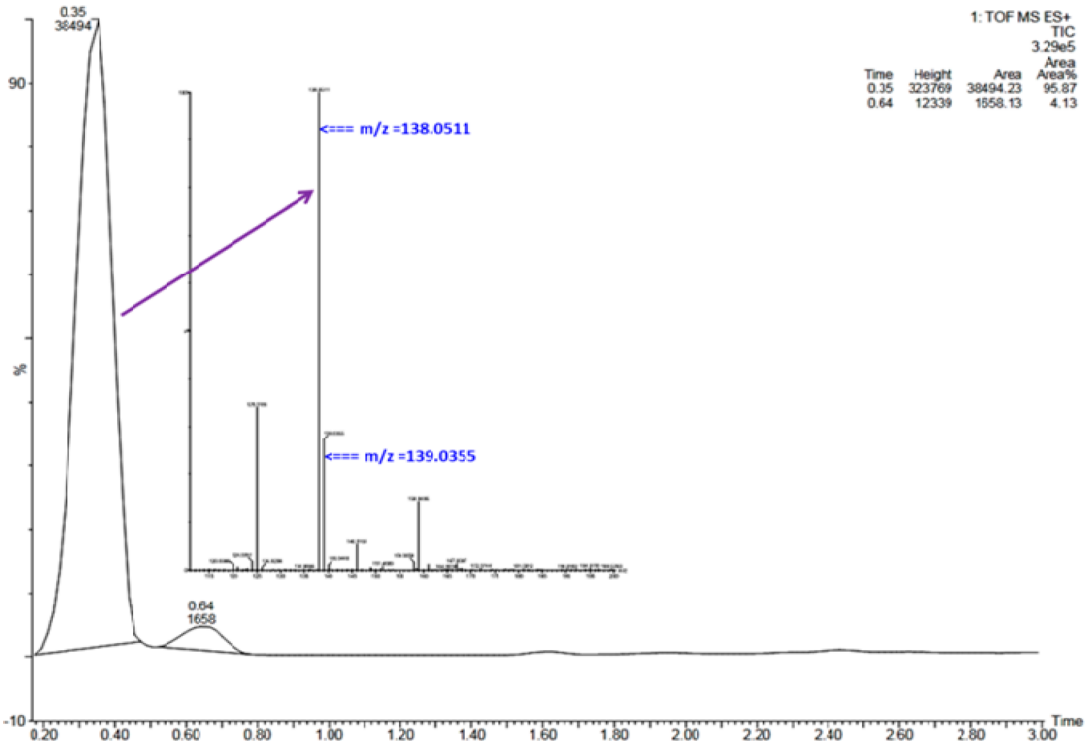

Figure 4. LC-MS spectra of methylimidate formed under identical reaction conditions in the presence of Mn^{II}.

phenomena features, probably a consequence of the expected low antiferromagnetic interaction attributable to the μ-$_{1,3}$ azide bridges, which is evidenced by the low position (12 K) of the susceptibility maximum.

The $\chi_M T$ product (Supporting Information, Figure S19) for compound **2a** shows a practically constant value of 0.41 cm^3 mol^{-1} K, which corresponds to one S = 1/2 with a g value of 2.09. Magnetization measurements show a constant increase of magnetization up to a maximum value equivalent to one electron under the maximum applied field of 5 T. The susceptibility measurements evidence that the Cu^{II} centers are magnetically isolated and in good agreement with the magnetization plot fitting perfectly to a Brillouin function for S = 1/2 and g = 2.11. Despite the 2D arrangement of the paramagnetic centers, this result becomes fully reasonable in light of the structural parameters: all possible superexchange pathways consisting of tetrazole bridges link equatorial coordination sites of

DOI: 10.1021/acs.inorgchem.5b01061
Inorg. Chem. 2015, 54, 7030−7037

one Cu^{II} cation with the axial coordination sites (nonmagnetic filled d-orbitals) of its neighbor.

Catalytic Studies and Mechanism of Formation of Methylimidate. We performed the reaction of 2-CN-Pym and sodium azide in 1:2 mol ratio in methanolic medium, in presence of catalytic amount of metal ions (M^{2+} = Mn^{2+} or Co^{2+}) for 20 h at 60 °C on an oil bath. Then, the reaction mixture was chromatographed over neutral alumina using *n*-hexane−ethyl acetate mixture as the eluent to separate the metal ion from the organic products. The organic products were analyzed by LC-MS using UPLC BEH-C18 (2.1 × 50 mm, 1.7 μm) column and 0.1% formic acid in water as solvent A and MeCN as solvent B. Analysis of elution peaks was performed by using Masslynx software. It was observed that when we used Mn^{II} as catalyst the conversion is almost 100% with methylimidate selectivity of 96% (Figure 4) with no sign of formation of tetrazole. However, when Co^{II} is used as catalyst, though the conversion is ∼100%, the methylimidate selectivity is only 60% along with the formation of tetrazole (∼36%; Supporting Information, Figure S6).

To ascertain the mechanism of the formation of complex **1**, we performed three reactions in solution phase and examined the products by means of ESI-MS^+(m/z) mass spectra analyses. As reported earlier, alkylimidate formation takes place only in presence of the corresponding alkoxide ion, and we also confirmed this by reacting 2-CN-Pym in MeOH in presence of catalytic amount of NaOMe, which gives the methylimidate ($C_6H_7N_3O$, MW = 137) (**3**), but the alkylimidate can also be formed by the Mn^{II}-catalyzed reactions between 2-CN-Pym and azide in MeOH in absence of any base (Supporting Information, Figure S7c). The formation of alkylimidate is confirmed by the X-ray analysis of complex **1** as well as by ESI-MS^+ of the products formed in situ in a reaction among 2-CN-Pym, NaN_3, and Mn^{II} in 2:4:1 mol ratio (Supporting Information, Figure S7a). Here, the reaction between 2-CN-Pym and NaN_3 leads to the formation of intermediate ($\mathbf{I_1}$). This is on coordination to a metal ion like Mn^{II} or Co^{II} gives intermediate $\mathbf{I_2}$. On coordination to a metal ion (Mn^{II} or Co^{II}) the carbon atom in (NaN_3^+−C═N^-) becomes electron defficient and thereby facilitates the nucleophilic attack by methanol, which subsequently loses the H^+ to C═N^- to form C═NH and cleaves the C−N (azide) bond leading to the formation of methylimidate. This process is facile only in presence of Mn^{II} ion, which can trap the methylimidate through complexation to form **1**. Therefore, the formation of methoxide ion from methanol is the driving force for the formation of methylimidate. The catalytic role of Mn^{II} is confirmed by performing the same reaction under identical conditions only in the absence of Mn^{II} or Co^{II} ions, which leads to the formation of tetrazole (**2**) as a sodium salt ($C_5H_3N_6Na$, MW = 170). The expulsion of N_3^- by MeO^- may be facile because MeO^- is a stronger nucleophile than N_3^-. The ESI-MS^+(m/z) of products **1**−**3** are given in Supporting Information, Figure S7. Thus, the proposed mechanism explains the formation of methylimidate in presence of Mn^{II} or Co^{II} salts (Scheme 5) as catalyst and proceeds through the nucleophilic attack of methoxy group from MeOH in competition with NaN_3 as another nucleophile. To generalize our observation we further extended our studies with several other aromatic nitriles (Supporting Information, Scheme S1), and the results are listed in Table 5. It was observed that Mn^{II} and Co^{II} lead to methylimidate as the major product, while other metals lead to the formation of tetrazoles as the only product.

CONCLUSIONS

The discovery of base-catalyzed formation of alkyl imidates through the addition of alcohols to nitriles dates back to 1895. Later on several nitriles with ethanol in the presence of sodium ethoxide were investigated to a considerable extent, which clearly established that the reactions are alkoxide-catalyzed and that the imidate formation was promoted by the presence of electron-withdrawing groups in the nitriles. Though the reaction condition is favorable for the click reaction, as evidenced from the reactions in the absence or presence of metal ions like Fe^{II}, Ni^{II}, Cu^{II}, and Zn^{II} (Supporting Information, Figures S8−S13) leading to the formation of tetrazole, methylimidate is formed in quantitative yield when Mn^{II} and Co^{II} are used as catalysts. The catalytic nature of this transformation reaction was confirmed by performing these experiments under catalytic conditions and analyzing the products using LC-MS techniques, which clearly showed almost 100% conversion and 96% and 60% selectivity in methylimidate in the presence of Co^{II} and Mn^{II} as catalysts, respectively. A tentative mechanism has been proposed for this unexpected transformation based on the structural and spectrometric results. So the present finding extends to metal ion-catalyzed formation of methylimidate in alcoholic medium without any alkoxide ions. Not only that, we have been successful in isolating and structurally characterizing a Mn^{II} complex (**1**) of the methylimidate ligand that exhibits a topology of 2D network of uninodal 3-c net with Schläfli symbol $\{6^3\}$ and also a 2D Cu^{II}-tetrazole complex (**2a**) and 1D Na^{I}-tetrazole (**2b**) complexes are formed from the same solution. The plot of $\chi_M T$ versus T with a well-defined maximum at 12 K clearly evidences overall anti-ferromagnetic character for compound **1**, whereas negligible coupling, due to axial−equatorial interactions, is found for the copper complex **2a**.

Scheme 5. Proposed Catalytic Cycle for the Formation of Methylimidate

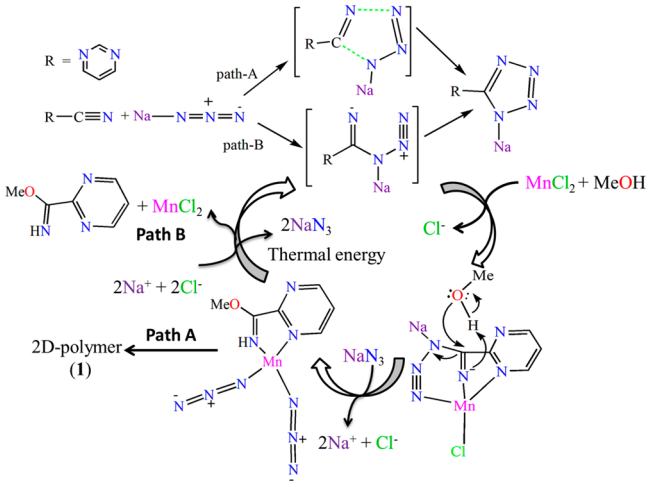

Table 5. Catalytic Transformation of Some Nitriles to Methylimidates in Presence of Mn^{II}/Co^{II} Metal as Catalyst

reagent	catalyst (metal center M^{2+})	product	% conversion	Figure
2-CN-Pym	Mn	methylimidate	95.87	4
2-CN-Pym	Co		60	S6
2-CN-Py	Mn	methylimidate	77.55	S14
2-CN-Py	Co		99.09	S15
benzontrile	Mn	methylimidate	56.46	S16
benzyl cyanide	Mn	methylimidate	69.20	S17
benzyl cyanide	Co		82.28	S18

ASSOCIATED CONTENT

Supporting Information

Illustrated 2D polyhedral network of complexes **1** and **2**, molecular view of H-bonded supramolecular architecture,

DOI: 10.1021/acs.inorgchem.5b01061
Inorg. Chem. 2015, 54, 7030−7037

powder XRD patterns, 1D molecular view of complex **2b**, HRMS (ESI-MS$^+$) spectra on the catalytic criteria of other metal, LC-MS spectra of Co^{II}/Mn^{II} catalysis, gradient program for UPLC-MS studies, selected bond distances and angles associated with hydrogen bonding in complex **1**, illustration of proposed catalytic cycle, and crystallographic information in the format of two CIF files. The Supporting Information is available free of charge on the ACS Publications website at DOI: 10.1021/acs.inorgchem.5b01061.

AUTHOR INFORMATION

Corresponding Author

*E-mail: m_ali2062@yahoo.com.

Notes

The authors declare no competing financial interest.

ACKNOWLEDGMENTS

Financial support from CSIR (Ref. No. 02(2490)/11/EMR-II) and UGC (Ref. No. UGC [39-735/2010(SR)], New Delhi, are gratefully acknowledged. M.D. thanks UGC (NET), New Delhi, for SRF fellowship. A single-crystal X-ray diffraction facility from Departmental DST-FIST program, Jadavpur University, is gratefully acknowledged. A.E. is thankful for support from CICYT Project No. CTQ2012-30662.

REFERENCES

(1) (a) Butler, R. N. In *Comprehensive Heterocyclic Chemistry;* Katritzky, A. R., Rees, C. W., Scriven, E. F. V., Eds.; Pergamon: Oxford, U.K., 1996; Vol. *4*.

(2) Himo, F.; Demko, Z. P.; Noodleman, L.; Sharpless, K. B. *J. Am. Chem. Soc.* **2002**, *124*, 12210−12216 and the references therein.

(3) Singh, H.; Chawla, A. S.; Kapoor, V. K.; Paul, D.; Malhotra, R. K. *Prog. Med. Chem.* **1980**, *17*, 151−183.

(4) (a) Ostrovskii, V. A.; Pevzner, M. S.; Kofmna, T. P.; Shcherbinin, M. B.; Tselinskii, I. V. *Targets Heterocycl. Syst.* **1999**, *3*, 467−526. (b) Hiskey, M.; Chavez, D. E.; Naud, D. L.; Son, S. F.; Berghout, H. L.; Bome, C. A. *Proc. Int. Pyrotech. Semin.* **2000**, *27*, 3−14.

(5) Koldobskii, G. I.; Ostrovskii, V. A. *Usp. Khim.* **1994**, *63*, 847−865.

(6) (a) Huisgen, R.; Sauer, J.; Sturm, H. J.; Markgraf, J. H. *Chem. Ber.* **1960**, *93*, 2106−2124. (b) Moderhack, D. *J. Prakt. Chem.* **1988**, *340*, 687−709.

(7) Mukhopadhyay, B. G.; Mukhopadhyay, S.; da Silva, M. F. C. G.; Charmier, M. A. J.; Pombeiro, A. J. L. *Dalton Trans.* **2009**, 4778−4785.

(8) (a) Quast, H.; Bieber, L. *Tetrahedron Lett.* **1976**, *18*, 1485−1486. (b) Krayushin, M. M.; Beskopylnyi, A. M.; Zlotin, S. G.; Lukyanov, O. A.; Zhulin, V. M. *Izv. Akad. Nauk. SSSR, Ser. Khim.* **1980**, *11*, 2668−2672. (c) Zavarzin, I. V.; Zhulin, V. M.; Yarovenko, V. N.; Krayushkin, M. M. *Izv. Akad. Nauk SSSR, Ser. Khim.* **1988**, *5*, 1168−1170. (d) Klaubert, D. H.; Sellstedt, J. H.; Guinosso, C. J.; Bell, S. C.; Capetola, R. J. *J. Med. Chem.* **1981**, *24*, 748−752. (e) Demko, Z. P.; Sharpless, K. B. *Angew. Chem.,Int. Ed.* **2002**, *12*, 2110−2113. (f) Demko, Z. P.; Sharpless, K. B. *Angew. Chem., Int. Ed.* **2002**, *12*, 2113−2116.

(9) Carpenter, W. R. *J. Org. Chem.* **1962**, *27*, 2085−2088.

(10) (a) Zhao, H.; Qu, Z.-R.; Ye, H.-Y.; Xiong, R.-G. *Chem. Soc. Rev.* **2008**, *37*, 84−100. (b) Zhang, X.-M.; Zhao, Y.-F.; Wu, H.-S.; Batten, S. R.; Ng, S. W. *Dalton Trans.* **2006**, 3170−3178. (c) Wang, X.-S.; Tang, Y.-Z.; Huang, X.-F.; Qu, Z.-R.; Che, C.-M.; Chan, P. W. H.; Xiong, R.-G. *Inorg. Chem.* **2005**, *44*, 5278−5285. (d) Xiong, R.-G.; Xue, X.; Zhao, H.; You, X.-Z.; Abrahams, B. F.; Xue, Z. *Angew. Chem., Int. Ed.* **2002**, *41*, 3800−3803.

(11) Lin, P.; Clegg, W.; Harrington, R. W.; Henderson, R. A. *Dalton Trans.* **2005**, 2388−2394.

(12) (a) Ellis, W. R., Jr.; Purcell, W. L. *Inorg. Chem.* **1982**, *21*, 834−837. (b) Paul, P.; Nag, K. *Inorg. Chem.* **1987**, *26*, 2969−2974. (c) Ziolo, R. F.; Thich, J. A.; Dori, Z. *Inorg. Chem.* **1972**, *11*, 626−631. (d) Gaughan, A. P.; Bowman, K. S.; Dori, Z. *Inorg. Chem.* **1972**, *11*, 601−608. (e) Kemmerich, T.; Nelson, J. H.; Takach, N. E.; Boebme, H.; Jablonski, B.; Beck, W. *Inorg. Chem.* **1982**, *21*, 1226−1232. (f) Sato, F.; Etoh, M.; Sato, M. *J. Organomet. Chem.* **1974**, *70*, 101−106.

(13) Pachfule, P.; Das, R.; Poddar, P.; Banerjee, R. *Cryst. Growth Des.* **2010**, *10*, 2475−2478.

(14) (a) Heme, B. C. *Am. Chem. J.* **1896**, *18*, 723−729. (b) Hessler, J. C. *Am. Chem. J.* **1899**, *22*, 169−198.

(15) (a) Stieglitz, J.; Schlesinger, H. I. *Am. Chem. J.* **1900**, *39*, 738−745. (b) Mckee, R. H. *Am. Chem. J.* **1901**, *26*, 209−217.

(16) (a) Marshall, E. K., Jr.; Acree, S. F. *Am. Chem. J.* **1913**, *49*, 127−158. (b) Marshall, E. K., Jr.; Harrison, J. P.; Acree, S. F. *Am. Chem. J.* **1913**, *49*, 369−405.

(17) Bayliss, N. S.; Heppolette, R. L.; Little, L. H.; Miller, J. *J. Am. Chem. Soc.* **1956**, *78*, 1978−1981.

(18) Schaefer, F. C.; Peters, G. A. *J. Org. Chem.* **1961**, *26*, 412−418 and references therein.

(19) Norris, R. O. U. S. Patent 1951, *2*, 569, 425−428.

(20) (a) Cramer, F.; Pawelzik, K.; Baldauf, H. *Chen. Ber.* **1958**, *91*, 1049−1054. (b) Steinkopf, W. *Ber.* **1907**, *40*, 164.3; **1920**, *53B*, 1149−1152. (c) Houben, J.; Kauffmann, H. *Ber.* **1913**, *46*, 2831−2837.

(21) *SMART (V 5.628), SAINT (V 6.45a), XPREP, SHELXTL;* Bruker AXS Inc.: Madison, WI, 2004.

(22) Sheldrick, G. M. *SADABS (Version 2.03);* University of Gottingen: Germany, 2002.

(23) Sheldrick, G. M. *Acta. Crystallogr.* **2008**, *A64*, 112−122.

(24) Spek, A. L. *Acta Crystallogr.* **2009**, *D65*, 148−155.

(25) (a) Blatov, V. A.; Shevchenko, A. P.; Serezhkin, V. N. J. *Appl. Crystallogr.* **2000**, *33*, 1193−1193. (b) Blatov, V. A.; Carlucci, L.; Ciani, G.; Proserpio, D. M. *CrystEngComm* **2004**, *6*, 378−395.

(26) Rodríguez-Diéguez, A.; Salinas-Castillo, A.; Galli, S.; Masciocchi, N.; Gutiérrez-Zorrilla, J. M.; Vitoria, P.; Colacio, E. *Dalton Trans.* **2007**, 1821−1828.

(27) Farrugia, L. J. *J. Appl. Crystallogr.* **1999**, *32*, 837−838.

(28) (a) Escuer, A.; Vicente, R.; Goher, M. A. S.; Mautner, F. A. *Inorg. Chem.* **1996**, *35*, 6386−6391. (b) Escuer, A.; Esteban, J.; Perlepes, S. P.; Stamatatos, T. C. *Coord. Chem. Rev.* **2014**, *275*, 87−129.

(29) Escuer, A.; Cano, J.; Journaux, Y.; Lloret, F.; Goher, M. A. S.; Mautner, F. A.; Vicente, R. *Inorg. Chem.* **2000**, *39*, 4688−4695.

(30) Li, X.-B.; Ma, Y.; Zhang, X.-M.; Zhang, J.-Y.; Gao, E.-Q. *Eur. J. Inorg. Chem.* **2011**, 4738−4744.

(31) (a) Youssef, M. A.; Escuer, A.; Goher, M. A. S.; Mautner, F. A.; Vicente, R. *J. Chem. Soc., Dalton Trans.* **2000**, 413−416. (b) Gao, E.-Q.; Bai, S.-Q.; Wang, Z.-M.; Yan, C.-H. *J. Am. Chem. Soc.* **2003**, *125*, 4984−4985. (c) Shen, Z.; Zuo, J.-L.; Yu, Z.; Zhang, Y.; Bai, J.-F.; Che, C.-M.; Fun, H.-K.; Vittal, J. J.; You, X.-Z. *J. Chem. Soc., Dalton Trans.* **1999**, 3393−3397. (d) Jia, Q.-X.; Tian, H.; Zhang, J.-Y.; Gao, E.-Q. *Chem.—Eur. J.* **2011**, *17*, 1040−1051.

(32) Escuer, A.; Mautner, F. A.; Goher, M. A. S.; Abu-Youssef, M. A. M.; Vicente, R. *Chem. Commun.* **2005**, 605−607.

(33) Gao, E.-Q.; Yue, Y.-F.; Bai, S.-Q.; He, Z.; Yan, C.-H. *J. Am. Chem. Soc.* **2004**, *126*, 1419−1429.

(34) Munno, G. D.; Julve, M.; Viau, G.; Lloret, F.; Faus, J.; Viterbo, D. *Angew. Chem., Int. Ed. Engl.* **1996**, *35*, 1807−1810.

(35) Kar, P.; Drew, M. G. B.; Gómez-García, C. J.; Ghosh, A. *Inorg. Chem.* **2013**, *52*, 1640−1649.

DOI: 10.1021/acs.inorgchem.5b01061
Inorg. Chem. 2015, 54, 7030−7037